DOI: 10.3901/CJME.2015.1023.126, available online at www.springerlink.com; www.cjmenet.com

Nondestructive Testing and Characterization of Residual Stress Field Using an Ultrasonic Method

SONG Wentao[1, 2], XU Chunguang[1], PAN Qinxue[1, *], and SONG Jianfeng[1]

1 *School of Mechanical Engineering, Beijing Institute of Technology, Beijing 100081, China*
2 *School of Mechanical Engineering, Shijiazhuang Tiedao University, Shijiazhuang 050043, China*

Received May 11, 2015; revised October 9, 2015; accepted October 23, 2015

Abstract: To address the difficulty in testing and calibrating the stress gradient in the depth direction of mechanical components, a new technology of nondestructive testing and characterization of the residual stress gradient field by ultrasonic method is proposed based on acoustoelasticity theory. By carrying out theoretical analysis, the sensitivity coefficients of different types of ultrasonic are obtained by taking the low carbon steel(12%C) as a research object. By fixing the interval distance between sending and receiving transducers, the mathematical expressions of the change of stress and the variation of time are established. To design one sending-one receiving and oblique incidence ultrasonic detection probes, according to Snell law, the critically refracted longitudinal wave (L_{CR} wave) is excited at a certain depth of the fixed distance of the tested components. Then, the relationship between the depth of L_{CR} wave detection and the center frequency of the probe in Q235 steel is obtained through experimental study. To detect the stress gradient in the depth direction, a stress gradient L_{CR} wave detection model is established, through which the stress gradient formula is derived by the relationship between center frequency and detecting depth. A C-shaped stress specimen of Q235 steel is designed to conduct stress loading tests, and the stress is measured with the five group probes at different center frequencies. The accuracy of ultrasonic testing is verified by X-ray stress analyzer. The stress value of each specific depth is calculated using the stress gradient formula. Accordingly, the ultrasonic characterization of residual stress field is realized. Characterization results show that the stress gradient distribution is consistent with the simulation in ANSYS. The new technology can be widely applied in the detection of the residual stress gradient field caused by mechanical processing, such as welding and shot peening.

Keywords: ultrasonic, nondestructive testing, acoustoelasticity theory, residual stress field, stress gradient, ultrasonic characterization

1 Introduction

Residual stress is a type of inherent stress that maintains stress balance in the inner material when the components are unaffected by external strength. The main sources of residual stress are mechanical processes, such as extrusion, rolling, drawing, correction, cutting, grinding, surface rolling, shot peening and hammering, as well as hot working including welding and cutting. Residual stress is usually harmful. For example, resistance to fatigue strength, brittleness fracture, stress corrosion cracking, and the stability of the size and shape of the components are significantly reduced under the combined action of residual stress, working temperature, and working medium[1–5]. Therefore, developing an effective detecting method is important in improving the residual stress state in the components.

Since the introduction of residual stress detecting technology in the 1930s, over 10 types of detection methods have been developed. Damage detection methods can be categorized into three, namely, destructive, half-destructive, and nondestructive methods[6–7]. Destructive testing methods include the slice and contour methods. Half-destructive methods include the blind hole, ring core, and deep hole methods. Nondestructive testing methods include the X-ray diffraction, neutron diffraction, magnetic measurement, and ultrasonic methods. The destructive and half-destructive testing methods belong to the category of stress release, and they more or less lead to the damage of tested component. The damage in service conditions of mechanical components is fatal and must be avoided. Therefore, nondestructive testing methods are more widely used. However, testing and calibrating the stress gradient in the depth direction of mechanical components using nondestructive testing methods are still difficult at present. For example, MIAO et al[8], measured residual stress in the precipitation-hardening layer of NAK80 steel before and after a shot peening treatment by X-ray diffraction method. The shot peening experiment results show that the depth of residual stress in the precipitation-hardening layer can reach approximately 450

* Corresponding author. E-mail: 18810328150@163.com
Supported by National Natural Science Foundation of China(Grant No. 51275042)

μm. However, the X-ray diffraction method can only detect a shallow residual stress field(5–20 μm). Hence, the author had to use numerical calculation to obtain a larger depth residual stress field. Neutron diffraction has a strong penetrating power(the maximum depth can reach 30 cm especially for the heavy metal). Thus, WITHERS[9] mapped residual and internal stress in hexagonal polycrystalline materials by neutron diffraction. However, building and running neutron reactors can be costly, thus limiting their practical applications in the industrial field. Magnetic measurement is also called Barkhausen noise method. On the basis of Barkhausen noise effect, DESVAUS, et al[10], inspected the homogeneity of surface and subsurface (in the first 60 μm under the surface) stresses on the bearing rings. Their result shows that magnetic measurement can only test the stress profile in the surface. Ultrasonic method has been rapidly developed. Different types of ultrasonic testing methods have been developed, such as the ultrasonic longitudinal wave[11], ultrasonic shear wave[12], combination of shear wave and longitudinal wave[13], ultrasonic surface wave[14], ultrasonic guided wave[15], nonlinear ultrasonic[16], and ultrasonic critically refracted longitudinal wave(L_{CR} wave)[17] methods. However, the residual stress gradient detection in the depth direction of mechanical components by ultrasonic method has yet to be reported.

To solve the aforementioned problem, the relationship between velocity and the direction of ultrasonic propagation and stress based on acoustoelasticity theory is studied, the sensitivity of different types of ultrasonic stress is discussed, and the theory for producing an L_{CR} wave is analyzed in this paper. An oblique incidence one sending-one receiving detection probe is then designed. The L_{CR} wave excited by the probe is used to test the residual stress in components. The ultrasonic detecting gradient model is established to realize stress gradient detection in the depth direction, and the relationship between the ultrasonic frequency and penetration depth is used to develop the stress gradient formula. Finally, a C-shaped stress test specimen is designed to verify the ultrasonic characterization method of the residual stress field.

2 Testing Method for Acoustoelasticity Theory

Acoustoelasticity theory is one of the main basis for ultrasonic stress testing. Acoustoelasticity theory is based on the finite deformation of continuum mechanics to study the relationship between the elastic solid stress state and the macroscopic elastic wave velocity.

Based on the four basic assumptions of acoustoelasticity, the elastic wave formula (acoustoelasticity formula) in stress medium under initial coordinates can be obtained[18–20] using the following equation:

$$\frac{\partial}{\partial \boldsymbol{X}_J}\left[\left(\delta_{IK}\boldsymbol{t}^i_{JL}+\boldsymbol{C}_{IJKL}\right)\frac{\partial \boldsymbol{u}_K}{\partial \boldsymbol{X}_L}\right]=\rho^i\frac{\partial^2 \boldsymbol{u}_I}{\partial t^2}, \tag{1}$$

where δ_{IK} is Kronecker delta function; ρ^i is the density of the solid in the loading condition; $\boldsymbol{u}_I$ and $\boldsymbol{u}_K$ are the dynamic displacements; $\boldsymbol{X}_J$ and $\boldsymbol{X}_L$ are the particle position vectors; $\boldsymbol{C}_{IJKL}$ is the equivalent stiffness, which depends on the material constant and the initial displacement field; and $\boldsymbol{t}^i_{JL}$ is the Cauchy stress shown in the initial coordinates under the solid loading state.

In the case of homogeneous deformation, Eq. (1) can be simplified as follows:

$$(\boldsymbol{C}_{IJKL}+\delta_{IK}\boldsymbol{t}^i_{JL})\frac{\partial^2 \boldsymbol{u}_K}{\partial \boldsymbol{X}_J\partial \boldsymbol{X}_L}=\rho^i\frac{\partial^2 \boldsymbol{u}_I}{\partial t^2}. \tag{2}$$

When the solid is isotropic, Eq. (2) can be analytically expressed[21]. Therefore, the formula for the ultrasonic propagation velocity and stress in solid can be established in Cartesian coordinates[22].

(1) For the longitudinal wave propagating along the stress direction:

$$\rho_0 V_{111}^2=\lambda+2\mu+\frac{\sigma}{3\lambda+2\mu}\left[\frac{\lambda+\mu}{\mu}(4\lambda+10\mu+4m)+\lambda+2l\right]. \tag{3}$$

(2) For the longitudinal wave propagating perpendicular to the stress direction:

$$\rho_0 V_{113}^2=\lambda+2\mu+\frac{\sigma}{3\lambda+2\mu}\left[2l-\frac{2\lambda}{\mu}(\lambda+2\mu+m)\right]. \tag{4}$$

(3) For the shear wave with a propagation direction along the stress direction and a polarization direction perpendicular to the stress direction:

$$\rho_0 V_{131}^2=\mu+\frac{\sigma}{3\lambda+2\mu}\left(\frac{\lambda n}{4\mu}+4\lambda+4\mu+m\right). \tag{5}$$

(4) For the shear wave with propagation direction and the polarization directions both perpendicular to the stress direction:

$$\rho_0 V_{132}^2=\mu+\frac{\sigma}{3\lambda+2\mu}\left(m-\frac{\lambda+\mu}{2\mu}n-2\lambda\right). \tag{6}$$

(5) For the shear wave with a propagation direction perpendicular to the stress direction and a polarization direction parallel to the stress direction:

$$\rho_0 V_{133}^2=\mu+\frac{\sigma}{3\lambda+2\mu}\left(\frac{\lambda n}{4\mu}+\lambda+2\mu+m\right). \tag{7}$$

(6) For the surface wave with a propagation direction parallel to the stress direction:

$$[\lambda+\alpha_{11}\alpha_{21}(\lambda+2\mu)]\left[1-\frac{(2\lambda+\mu)\sigma}{(3\lambda+2\mu)\mu}\right]+\lambda\left(1+\frac{\sigma}{\mu}\right)=0, \tag{8}$$

where $\alpha_{11}=\left[1-(V_{11}/V_{1L})^2\right]^{1/2}$; $\alpha_{21}=\left[1-(V_{11}/V_{1S})^2\right]^{1/2}$; and V_{1L} and V_{1S} are the velocity of the longitudinal wave and the shear wave under the condition of free stress in a solid, respectively.

(7) For the surface wave with a propagation direction perpendicular to the stress direction:

$$[\lambda+\alpha_{12}\alpha_{22}(\lambda+2\mu)]\left[1-\frac{(2\lambda+\mu)\sigma}{(3\lambda+2\mu)\mu}\right]+\lambda\left(1+\frac{\sigma}{\mu}\right)=0, \tag{9}$$

where $\alpha_{12}=\left[1-(V_{12}/V_{1L})^2\right]^{1/2}$, $\alpha_{22}=\left[1-(V_{12}/V_{1S})^2\right]^{1/2}$.

In Eqs. (3)–(9), λ and μ are the second-order elastic constants; l,m,n are the third-order elastic constants; ρ_0 is the density of the solid before deformation; and σ is the stress applied in one direction (tensile stress is positive and compressive stress is negative). The velocities of the longitudinal wave and shear wave are expressed by three subscripts (e.g., V_{ABC}). The first, second, and third subscripts express the wave propagation direction, the particle polarization direction and the direction of the stress, respectively. The velocities of the surface wave are expressed by two subscripts (e.g., V_{AB}). The first subscript expresses the direction of wave propagation, and the second subscript expresses the direction of the stress.

The wave velocity V derivative of stress σ in Eqs. (3)–(9) are selected and $\mathrm{d}V=K_\alpha \mathrm{d}\sigma$ is obtained, where K_α is the stress sensitivity coefficient. A larger value of $|K_\alpha|$ indicates that the wave is more sensitive to stress.

The elastic constants of common materials are shown in Table 1[23].

Table 1. Second-order and third-order constants of the materials GPa

Material	λ	μ	l	m	n
Steel (0.12%C)	115	82	–301±37	–666±6.5	–716±4.5
Aluminium (99%)	61±1	25	–47±25	–342±10	–248±10
Copper (99.9%)	104	46	–542±30	–372±5	–401±5

To obtain the stress sensitivity coefficients of different types of ultrasonic, the low carbon steel (0.12%C) is chosen as an example. The density of steel is 7.85 g/cm^3, the velocity of ultrasonic in free stress is V_{111}=V_{113}=5.90 km/s, V_{131}=V_{132}=V_{133}=3.20 km/s. By plugging these values into the formulas, the following results are obtained:

$$\begin{aligned}&\mathrm{d}V_{111}\approx-0.080\ 85\,\mathrm{d}\sigma,\quad \mathrm{d}V_{113}\approx0.010\ 25\,\mathrm{d}\sigma,\\&\mathrm{d}V_{131}\approx-0.005\ 05\,\mathrm{d}\sigma,\quad \mathrm{d}V_{132}\approx-0.005\ 05\,\mathrm{d}\sigma,\\&\mathrm{d}V_{133}\approx-0.024\ 95\,\mathrm{d}\sigma.\end{aligned} \tag{10}$$

The relationship between surface wave and stress is complex and nonlinear, which is related to the transverse wave and longitudinal wave velocity under the solid material stress state, the wave velocity of the surface wave, and the stress values. When the stress values are σ=100 MPa, and V_{11}=3.0 km/s, V_{1L}=5.9 km/s, V_{1S}=3.2 km/s, the following results can be obtained:

$$\mathrm{d}V_{11}\approx\mathrm{d}V_{12}\approx-0.001\ 53\,\mathrm{d}\sigma. \tag{11}$$

Hence, Fig. 1 is obtained by comparing the stress sensitivity coefficients of various wave types. As shown in the diagram, the longitudinal wave propagating along the stress direction is the most sensitive to stress, thus facilitating tangential residual stress wave detection.

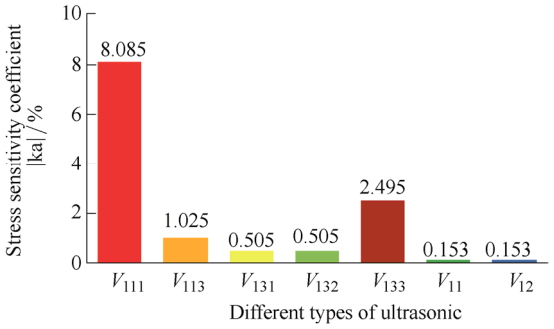

Fig. 1. Stress sensitivity coefficient |Ka| of different types of ultrasonic

3 Testing Principle of the L_{CR} Wave

According to the Snell law, when a longitudinal wave propagates from a medium (in which the wave velocity is slower) to another medium (in which the wave velocity is faster) an incidence angle exists (θ_{Lcr}), which makes the refraction angle of the longitudinal wave (θ_L) equal to 90°. A longitudinal wave with a refraction angle equal to 90° is called the L_{CR} wave. The angle of incidence is the first critical angle. Taking a PMMA acoustic wedge and Q235 steel component for example, as shown in Fig. 2, the first critical angle of the component is defined as follows:

$$\theta_{Lcr}=\arcsin(V_1/V_2). \tag{12}$$

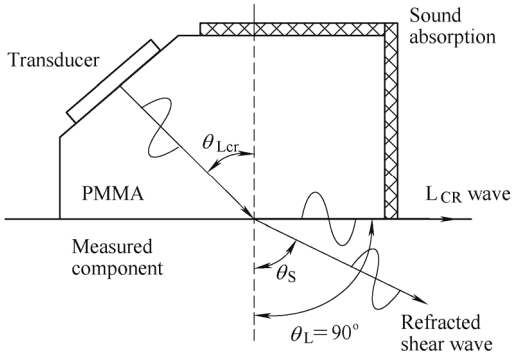

Fig. 2. Mechanism of the L_{CR} wave

The L_{CR} waves propagating along the specimen surface are stress-sensitive, have low attenuation, and tend to spread fast. Their signal analysis positioning is relatively simple, which is suitable for the detection of residual stress. If the frequency of the fixed transducer is known, then the value of residual stress at the corresponding penetrating depth can be detected.

According to the study of acoustoelasticity theory, the relationship between the longitudinal wave velocity propagating along the stress direction and the stress is obtained, as shown in Eq. (3). In practical detection, the distance between the sending and receiving transducer is fixed. The change of the sound velocity can be determined by calculating the change of the sound time. Accordingly, the acoustic elastic effect can be obtained. On the basis of Eq. (3), the relationship between the stress variation and the time change of sound propagation can be obtained as follows:

$$\mathrm{d}\sigma = K_S \mathrm{d}t, \quad K_S = -\frac{2}{K_\alpha t_0}, \tag{13}$$

where K_S is the stress coefficient, and t_0 is the time it takes for the longitudinal wave to propagate over a fixed distance under the condition of zero stress.

4 Principle of Residual Stress Gradient Testing

By using oblique incidence method, an L_{CR} wave is excited from a one sending-one receiving probe at a certain depth of fixed distance in the measured component, as shown in Fig. 3. The penetration depth of the L_{CR} wave is considered as a function of its frequency when the L_{CR} wave propagates in a component with finite thickness; however, no exact theoretical formula is known to reflect the relationship between the penetration depth of the L_{CR} wave and its frequency[24–26]. The experiment research shows that the detection depth D changes quantitatively as the center frequency of the excitation and receiving transducer changes. As shown in Fig. 4, the relationship between the depth and the frequency satisfies the following empirical equation[27]:

$$D = V \times f^{-0.96}, \tag{14}$$

where D is the penetration depth of the L_{CR} wave (mm), f is the sending/receiving frequency of the ultrasonic transducer(MHz), and V is the velocity of the L_{CR} wave in the component(km/s).

An ultrasonic testing model of the residual stress gradient is also established. To simplify the model, the ultrasonic testing area is considered a rectangle area, as shown in Fig. 5.

The corresponding detection depths of ultrasonic transducer frequencies f_1, f_2, f_3 are D_1, D_2, D_3, and the relationship between each pair is shown in Eq. (14). The corresponding residual stress detection values of ultrasonic transducer frequencies f_1, f_2, f_3 are $\sigma_1, \sigma_2, \sigma_3$. To determine the residual stress σ_{1-2} at the depth D_{1-2}, the following formula can be used:

$$\sigma_{1-2} = \frac{\sigma_2 \times (D_2 Ld) - \sigma_1 \times (D_1 Ld)}{D_2 Ld - D_1 Ld}. \tag{15}$$

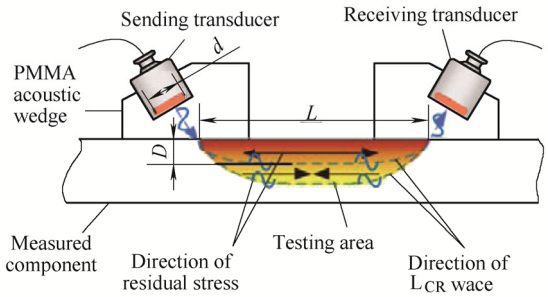

Fig. 3. Principle of stress gradient testing

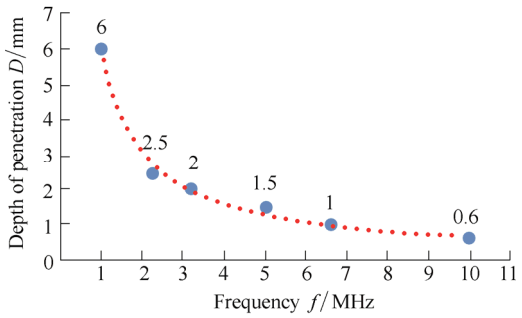

Fig. 4. Relationship between the penetration depth and the frequency of the L_{CR} wave
(The tested component is Q235 steel, the velocity of the L_{CR} wave V is 5.9 km/s, and the crystal dimension d is 6 mm)

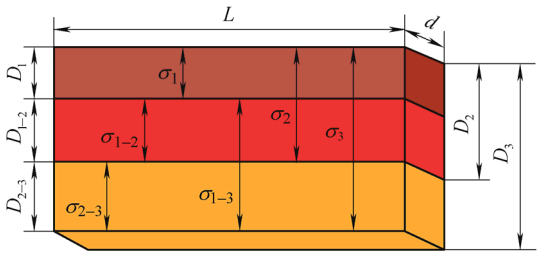

Fig. 5. Ultrasonic testing model of the residual stress gradient

The sound path L and the diameter d of the transducer are usually unchanged. Accordingly, Eq. (15) can be simplified as follows:

$$\sigma_{1-2} = \frac{\sigma_2 D_2 - \sigma_1 D_1}{D_2 - D_1}. \tag{16}$$

Similarly, the residual stress σ_{2-3} at the depth D_{2-3} can be obtained using the following equation:

$$\sigma_{2-3} = \frac{\sigma_3 D_3 - \sigma_2 D_2}{D_3 - D_2}. \tag{17}$$

By analogy, if the frequencies of the ultrasonic transducer are $f_1, f_2, \cdots, f_n$ from high to low, then the corresponding detection depths are $D_1, D_2, \cdots, D_n$. The residual stress σ_{i-j} at arbitrary depth D_{i-j} can be calculated using the following equation:

$$\sigma_{i-j} = \frac{\sigma_j D_j - \sigma_i D_i}{D_j - D_i}. \tag{18}$$

By plugging Eq. (14) into Eq. (18), the relationship between the depth of the residual stress gradient and the frequency can be obtained as follows:

$$\sigma_{i-j} = \frac{\sigma_j f_j^{-0.96} - \sigma_i f_i^{-0.96}}{f_j^{-0.96} - f_i^{-0.96}}. \tag{19}$$

5 Ultrasonic Characterization of the Residual Stress Field

A C-shaped stress test specimen is designed to produce simple and accurate stress. The material is Q235 steel with an external diameter of 137 mm and thickness of 5 mm. The surface stress and the depth direction stress gradient can be obtained through the specimen. When the bolts are tightened, the outer ring produces tensile stress and the inner ring produces compressive stress, as shown in Fig. 6. The stress distribution of the surface and the depth direction are shown in Fig. 7 with the bolt inserted by 3 mm.

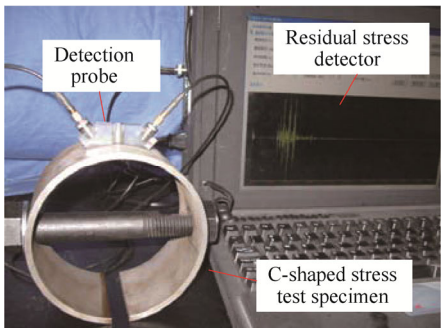

Fig. 6. Ultrasonic testing of the residual stress field

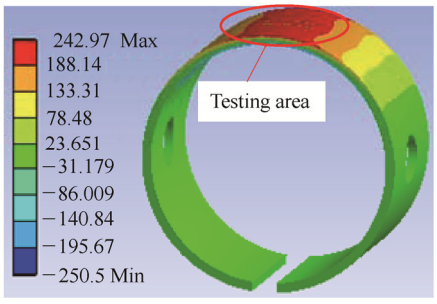

Fig. 7. Stress simulation of the C-shaped sample

Five group probes with the same sizes but different frequencies are used. The receiver circuitry of pulser/receiver board in the ultrasonic detector has high- and low-pass filter functions. The high-pass filters include six second-order passive Butterworth selections: 0.5, 2.0, 4.0, 8.0, 12.5, and 22.5 MHz. The low-pass filters also include six second-order passive Butterworth selections: 2.0, 5.0, 7.5, 12.5, 17.5, and 30 MHz. Considering that transducers generate a short pulse that contains a broad frequency range, the high- and low-pass filters should be used to obtain a specific range of frequencies. The parameters are shown in Table 2.

Table 2. Testing parameters of the different frequency transducers

Number	Centre frequency f/MHz	Detected depth D/mm	Crystal dimension /mm	High-low pass filters /MHz
1	15	0.44	6	12.5–17.5
2	10	0.65	6	8.0–12.5
3	5	1.26	6	4.0–7.5
4	4	1.56	6	2.0–5.0
5	2.5	2.45	6	0.5–5.0

To verify that the ultrasonic L_{CR} wave method is accurate and has high resolution, MSF-3M model X-ray stress analyzer made by Rigaku Corporation is used. The main parameters are shown in Table 3. Prior to conducting the experiment, the X-ray stress analyzer is used to detect stress in zero stress iron powder. The detection result is –0.62±2.12 MPa, indicating that the precision of the analyzer satisfies the requirements.

Table 3. Main parameters of the X-ray stress analyzer

Name	Parameter
Tube voltage	30 kV (fixed)
Tube current	0.5–10 mA (continuously adjustable)
X-ray type	Ka
Target	Cr
Focusing area	4 mm×4 mm

Residual stress is detected by using these five group probes and X-ray stress analyzer when the bolt is inserted by 0, 0.5, 1, 1.5, 2, 2.5, and 3 mm. The stress curve is shown in Fig. 8.

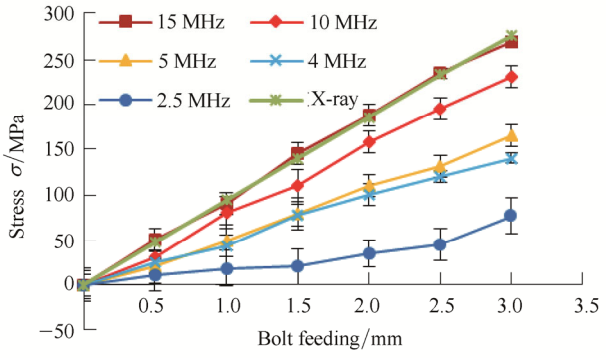

Fig. 8. Stress testing curve of the different frequency probes

As shown in Fig. 8, considering that the X-ray diffraction method can only detect surface residual stress, the stress value detected by the X-ray stress analyzer is the same as that detected by ultrasonic residual stress detector with a 15-MHz probe. Furthermore, the residual stress value detected by the high frequency transducer is larger than the residual stress value detected by the low frequency transducer under the same bolt feeding. This trend is consistent with the stress gradient of C-shaped specimen.

Taking a group of stress testing data at the bolt feeding of 3 mm as an example, the stress value of a certain depth at every state can be calculated using Eq. (19). Accordingly, the detection of residual stress gradient is realized (as shown in Table 4).

Table 4. Stress values tested by ultrasonic

No.	Frequency f/MHz	Feeding /mm	Detected depth D/mm	Stress value σ/MPa
1	15	3	0.44	268.8
2	10	3	0.65	230.5
3	5	3	1.26	165.8
4	4	3	1.56	140.1
5	2.5	3	2.45	76.6

The stress of each layer depth can be derived when the data in Table 4 are plugged into Eq. (19). The stress nephogram is shown in Fig. 9.

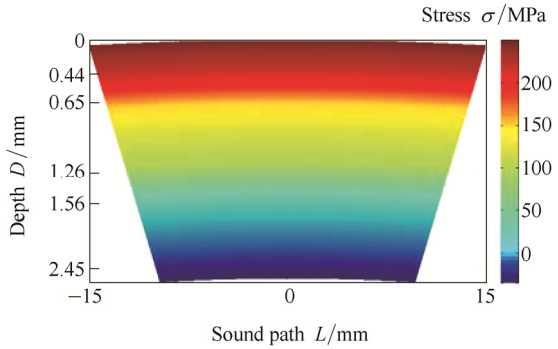

Fig. 9. Ultrasonic characterization of the stress gradient

The C-shaped specimen stress distribution chart at a depth of 2.45 mm is obtained via simulation, as shown in Fig. 10. Comparing Figs. 9 and 10, the stress gradient of the ultrasonic characterization method is consistent with the simulation result. The main error sources are as follows.

(1) Both the actual center frequency of the transducer and the given value have a minor deviation.

(2) The machining precision of the C-shaped specimen is not enough, and the simulation size is slightly different from the actual size.

(3) Bolt feeding in the practical operation has numerical reading errors.

(4) The ultrasonic testing error increases because of the change of the coupling layer thickness when C-shaped specimen surface curvature changes.

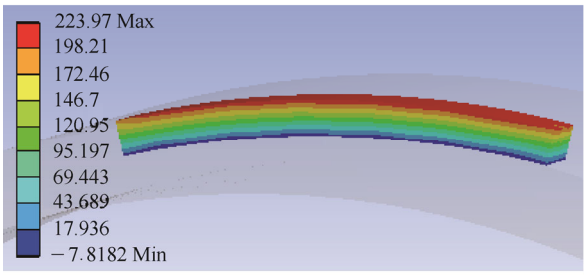

Fig. 10. Simulation of the stress gradient distribution

6 Conclusions

(1) Based on the ultrasonic acoustoelasticity theory, residual stress detection principles are analyzed. Taking the low carbon steel(0.12%C) as an example, the sensitivity coefficients of different types of ultrasonic are obtained. A comparison of the stress sensitivity coefficients shows that the longitudinal wave propagating along the stress direction is the most sensitive to stress. Thus, this method is suitable for residual stress testing.

(2) According to Snell law, the one sending-one receiving and oblique incidence ultrasonic detection probes are designed to excite the L_{CR} wave at a certain depth of the tested components. Through the relationship between the depth of L_{CR} wave detection and the center frequency, a stress gradient L_{CR} wave detection model is established and the stress gradient formula is presented.

(3) A C-shaped stress specimen of Q235 steel is designed to generate the stress gradient, which is measured with the five group probes at different center frequencies. The ultrasonic characterization of the residual stress field is realized using the stress gradient formula. The accuracy of ultrasonic testing is verified by X-ray diffraction method.

(4) The stress gradient distribution of the specimen is also obtained by ANSYS simulation. The results of ultrasonic characterization and the simulation are consistent. Therefore, this new technology can be widely applied to the detection of the residual stress gradient field caused by mechanical processing, such as welding and shot peening.

(5) Further studies should be developed on the influencing factors that affect the detection of the residual stress gradient field, such as inhomogeneity of measured material, accuracy of detection system, horizontal linearity of the instrument, the L_{CR} wave probe parameters, and the acoustic character. These factors are closely related to the accuracy and reliability of practical detection, and even to its engineering application promotion.

References

[1] LIU C, ZHUANG D. Internal welding residual stress measurement based on contour method[J]. *Chinese Journal of Mechanical Engineering*, 2012, 48(8): 54–59. (in Chinese)

[2] TOTTEN G E, HOWES M, INOUE T. *Handbook of residual stress and deformation of steel*[M]. New York: ASM International Publishers, 2002.

[3] CHAN K S, ENRIGHT M P, MOODY J P, et al. Residual stress profiles for mitigating fretting fatigue in gas turbine engine disks[J]. *International Journal of Fatigue*, 2010, 32: 815–823.

[4] ZAROOG O S, ALI A, SAHARI B B, et al. Modeling of residual stress relaxation of fatigue in 2024-T351 aluminium alloy[J]. *International Journal of Fatigue*, 2011, 33: 279–285.
[5] JACOMINO J L, BURGOS J S, CRUZ A C, et al. Use of explosives in the reduction of residual stresses in the heated zone of welded joints[J]. *Welding International*, 2010, 24(12): 920–925.
[6] WITHERS P J, BHADESHIA H K. Residual stress Part 1—Measurement techniques[J]. *Materials Science and Technology*, 2001, 17: 355–365.
[7] ROSSINI N S, DASSISTI M, BENYOUNIS K Y, et al. Methods of measuring residual stresses in components[J]. *Materials and Design*, 2012, 35: 572–588.
[8] MIAO H, ZUO D W, WANG M, et al. Numerical calculation and experimental research on residual stresses in precipitation-hardening layer of NAK80 steel for shot peening[J]. *Chinese Journal of Mechanical Engineering*, 2011, 24(3): 439–445.
[9] WITHERS P J. Mapping residual and internal stress in materials by neutron diffraction[J]. *Comptes Rendus Physique*, 2007, 8(8): 806–820.
[10] DESVAUS S, DUQUENNOY M, GUALANDRI J, et al. Evaluation of residual stress profiles using the Barkhausen noise effect to verify high performance aerospace bearings[J]. *Nondestructive Testing and Evaluation*, 2005, 20(1): 9–24.
[11] JHANG K Y, QUAN H H, HA J, et al. Estimation of clamping force in high-tension bolts through ultrasonic velocity measurement[J]. *Ultrasonics*, 2006, 44: e1339–e1342.
[12] SASAKI Y, HASEGAWA M. Effect of anisotropy on acoustoelastic birefringence in wood[J]. *Ultrasonics*, 2007, 46: 184–190.
[13] CHAKI S, COMELOUP G, LILLAMAND I, et al. Combination of longitudinal and transverse ultrasonic waves for in situ control of the tightening of bolts[J]. *Journal of Pressure Vessel Technology*, 2007, 129(3): 383–390.
[14] HU E Y, HE Y M, CHEN Y M. Experimental study on the surface stress measurement with Rayleigh wave detection technique[J]. *Applied Acoustics,* 2009, 70: 356–360.
[15] LIU Z H, LIU S, WU B, et al. Experimental research on acoustoelastic effect of ultrasonic guided waves in prestressing steel strand [J]. *Chinese Journal of Mechanical Engineering*, 2010, 46(2): 22–27. (in Chinese)
[16] LIU M, KIM J Y, JACOBS L, et al. Experimental study of nonlinear Rayleigh wave propagation in shot-peend aluminum plates—Feasibility of measuring residual stress[J]. *NDT&E International*, 2011, 44: 67–74.
[17] LU H, LIU X S, ZHU Z, et al. Rapid and nondestructive measurement system for welding residual stress by ultrasonic method[J]. *Chinese Journal of Mechanical Engineering*, 2008, 21(6): 91–93.
[18] HUGHES D S, KELLY J L. Second-Order elastic deformation of solids[J]. *Physics Review*, 1953, 92(5): 1145–1149.
[19] TATSUO T, YUKIO I. Acoustical birefringence of ultrasonic waves in deformed isotropic elastic materials[J]. *International Journal of Solids Structures*, 1968, 4: 383–389.
[20] PAO Y H, SACHSE W. Acoustoelasticity and ultrasonic measurement of residual stresses[J]. *Physical Acoustics*, 1984, 17: 62–140.
[21] BRAY D E, JUNGHANS P. Application of the Lcr ultrasonic technique for evaluation of post-weld heat treatment in steel plates[J]. *NDT&E International*, 1995, 28(4): 235–242.
[22] ROSE J L. *Ultrasonic waves in solid media*[M]. Cambridge: Cambridge University Press, 1999.
[23] VIKTOR H. *Structural and residual stress analysis by nondestructive methods*[M]. Netherlands: Elsevier Press, 1997.
[24] YASHAR J, MEHDI A, MEHDI A N, Using finite element and ultrasonic method to evaluate welding longitudinal residual stress through the thickness in austenitic stainless steel plates[J]. *Materials and Design*, 2013, 45: 628–642.
[25] YASHAR J, MEHDI A N, MEHDI A. Residual stress evaluation in dissimilar welded joints using finite element simulation and the L_{CR} ultrasonic wave[J]. *Russian Journal of Nondestructive Testing*, 2012, 48(9): 541–552.
[26] YASHAR J, HAMED S P, MOHAMMADREZA H R, et al. Ultrasonic inspection of a welded stainless steel pipe to evaluate residual stresses through thickness[J]. *Materials and Design*, 2013, 59: 591–601.
[27] SONG W T, PAN Q X, XU C G, et al. Residual stress nondestructive testing for pipe component based on ultrasonic method[C]//*2014 Far East Forum on Nondestructive Evaluation/Testing: New Technology & Application*, 2014: 163–167.

Biographical notes

SONG Wentao, born in 1986, is currently a PhD candidate at *School of Mechanical Engineering, Beijing Institute of Technology, China*. His research interests include nondestructive testing and regulation of residual stress.
Tel: +86-10-68918436; E-mail: 603745170@qq.com

XU Chunguang, born in 1964, is currently a professor at *Lab for NDT and Control, School of Mechanical Engineering, Beijing Institute of Technology, Beijing, China*. He received his PhD degree from *Beijing Institute of Technology, Beijing, China*, in 1995. His research interests include ultrasonic sound field theory, defect of automatic ultrasonic scanning, ultrasonic microscope, residual stress of ultrasonic testing, ultrasonic transducer performance measurement and calibration, metal defect shape ultrasonic array detection and recognition, composite nondestructive testing and evaluation techniques and theory.
E-mail: xucg@bit.edu.cn

PAN Qinxue received his PhD degree in intelligent mechannical engineering and system, *Kagawa University* in 2010. He is working at *School of Mechanical Engineering, Beijing Institute of Technology, China* since 2010. His research interests include NDT&E technology and residual stress measurement technology.
E-mail: +86-18810328150@163.com

SONG Jianfeng, born in 1992, is currently a master candidate at *Lab for NDT and Control, School of Mechanical Engineering, Beijing Institute of Technology, China.*
E-mail: +86-15827349393@163.com